Studies of Photoexcited States in Polyacetylene and Poly(paraphenylenevinylene) by Absorption Detected Magnetic Resonance: The Case of Neutral Photoexcitations

X. Wei, B. C. Hess,[a] and Z. V. Vardeny

Physics Department, University of Utah, Salt Lake City, Utah 84112

F. Wudl

Institute of Polymers and Organic Solids and Physics Department, University of California, Santa Barbara, California 93106

(Received 14 June 1991)

Photoexcited states in *trans* polyacetylene [t-$(CH)_x$] and in alkoxy derivatives of poly(paraphenylenevinylene) (PPV) have been studied by the technique of absorption detected magnetic resonance. In addition to the stable *charged* photoexcitations, which are charged solitons in t-$(CH)_x$ and bipolarons in PPV, we clearly identify *neutral* photoexcitations with *nonzero* spins. In t-$(CH)_x$ these are spin-$\frac{1}{2}$ neutral solitons S^0 ($\bar{S}^0$) with an optical transition at 1.35 eV. The neutral photoexcitations in PPV form triplet excitons which cannot dissociate into $S^0\bar{S}^0$ pairs due to the confinement caused by the nondegenerate backbone structure.

Photoexcited states and their relaxation processes in conducting polymers with degenerate and nondegenerate backbone ground-state structures have generated considerable experimental and theoretical studies in the last decade [1]. This has been stimulated by the possibility that various types of nonlinear excitations such as solitons, polarons, bipolarons, and breathers can be photogenerated [2]. Most of the studies, however, have been focused on *charged* photoexcitations because of the relatively easy comparison with available spectroscopic data on nonlinear excitations produced by doping [2], and more recently by field injection [3]. A relatively simple picture has emerged for charged photocarriers: They form solitons ($S^{\pm}$) in the degenerate polymer *trans* polyacetylene [t-$(CH)_x$], whereas in nondegenerate ground-state polymers, such as polythiophene and poly(paraphenylenevinylene) (PPV), photocarriers form polarons ($P^{\pm}$) and bipolarons ($BP^{2\pm}$); this picture is based on noninteracting model Hamiltonians, such as that of Su, Schrieffer, and Heeger (SSH) [4].

On the other hand, there is now accumulating experimental evidence [5–7] of the importance of the π-electron Coulomb interaction U in this class of conducting polymers, which places U at the intermediate level, 3 eV $< U <$ 7 eV. The reversed order of the even ($2A_g$) and odd (B_u) excited-state symmetries in short polyenes [8] is thought to result from the strong Coulomb correlation. Interestingly, more recent calculations of photoexcitations within interacting model Hamiltonians using nonperturbative [9–11] methods and numerical renormalization-group methods [12] show that *neutral* photoexcitations compete with charged excitations in the photophysics of conducting polymers. In this picture the lowest excited state ($2A_g$), if reached, decays into *triplet* neutral excitations; in degenerate ground-state polymers such as t-$(CH)_x$, the triplet excitations dissociate further [11] into spin-$\frac{1}{2}$ *neutral* soliton-antisoliton ($S^0\bar{S}^0$) pairs. Thus, in addition to the stable charged photoexcitations

predicted in the $U=0$ limit ($S^{\pm}$, $P^{\pm}$, and $BP^{2\pm}$) these models predict stable triplet ($S=1$) and doublet ($S=\frac{1}{2}$) neutral photoexcitations which may be observed with spin-sensitive experimental techniques.

In the present work we have applied such a spin-sensitive technique, absorption detected magnetic resonance (ADMR), to investigate the spin and charge states of photoexcitations in degenerate [t-$(CH)_x$] and nondegenerate (PPV) ground-state conducting polymers. In t-$(CH)_x$ we have found that the well-known 1.35-eV spectral feature [13] is associated with spin-$\frac{1}{2}$ neutral photoexcitations, which we identify as neutral solitons S^0. In alkoxy derivatives of PPV, on the other hand, we have identified both charged and neutral excited states. The charged photocarriers form $BP^{2\pm}$ with two optical transitions at 0.3 and 1.25 eV, respectively, which are a correlated bound pair of spin-$\frac{1}{2}$ $P^{\pm}$. The neutral photoexcitations, however, are triplet ($S=1$) excitons with an optical transition in the triplet manifold at 1.35 eV.

In ADMR we detect changes in the steady-state photomodulation (PM) spectrum associated with induced changes in the photoexcitation recombination kinetics. This is caused by resonant microwave absorption among Zeeman-split electronic energy levels in a moderately strong magnetic field. This technique is similar to another optical detected magnetic resonance, phosphorescence detected magnetic resonance (PDMR) [14], except that in ADMR, changes in PM intensity are detected, whereas in PDMR, changes in photoluminescence (PL) intensity are recorded.

Our ADMR setup consists of a pump beam, from an Ar^+ laser at 488 nm, and a probe beam from an incandescent light source dispersed by a monochromator. The sample was placed in a high-Q-value microwave cavity with resonance at about 3 GHz (S band), equipped with optical windows for transmission. The cavity was placed in a Dewar in a superconducting magnet with a field H up to 3 T. We used an rf field with power up to 200 mW

which was modulated at 500 Hz. After proper signal averaging, the sensitivity of our apparatus $\delta T/T$ (where T is the transmission and δT is its spin modulation) was $\delta T/T \simeq 3 \times 10^{-8}$ in the Si-detector spectral range, which decreased to 2×10^{-7} in the InSb ir range. Two types of ADMR and PDMR spectra were obtained: the H-ADMR spectrum for which H was swept at a fixed probe wavelength, and the P-ADMR spectrum for which the probe wavelength was changed at a constant H, in resonance. The samples studied were three Shirakawa polymerized t-$(CH)_x$ thin films and two solution-cast films of alkoxy derivatives of PPV:DOO [poly(2,5-octoxy-PV)] and DHO [poly(2,5-hexoxy-PV)] [15], all deposited on sapphire substrates.

The PM spectrum of t-$(CH)_x$ at 4 K is shown in Fig. 1. Two photoinduced absorption (PA) bands at 0.45 eV (LE) and at 1.35 eV (HE) dominate the PM spectrum [13]. The LE band was identified [2] as due to $S^{\pm}$; associated with it is a prominent oscillation above 1.4 eV, identified [16] as due to electroabsorption (EA) caused by $S^{\pm}$. The HE band, associated with neutral photoexcitations [16], however, has still remained a mystery for over a decade; singlet [17] and triplet [9] solitonic excitons, breather modes [18], and A_g states [16] are only a few of the explanations given for the HE band that can be found in the literature. The ADMR spectra shown in Fig. 1 can elucidate its origin. The H-ADMR signal at 1.35 eV (at the HE peak) is shown in Fig. 1 (inset). A reduction of PA ($\delta n < 0$), with $\delta n/n \simeq 3 \times 10^{-3}$, where n is the steady-state population and δn is its change, is observed at 1067 G ($S = \frac{1}{2}, g \simeq 2.003$). This is caused by enhanced recombination associated with the HE excitations with unthermalized spins. This eliminates the singlet excitons [17] and breather modes [18] for which $S = 0$, as
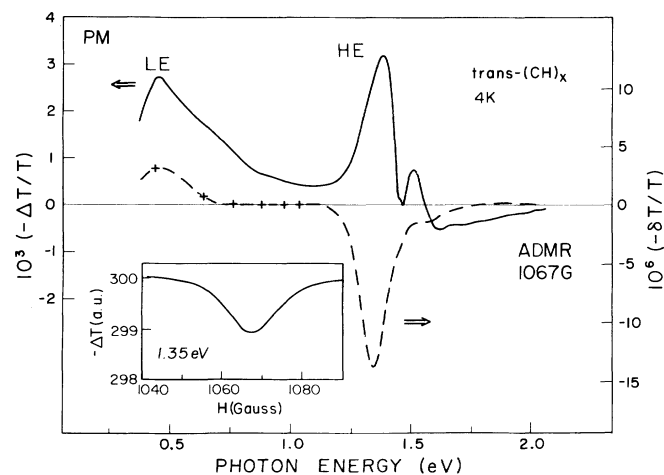
well as triplet excitons [9], as valid explanations for the HE band.

The P-ADMR spectrum of t-$(CH)_x$ at a fixed H of 1067 G is also shown in Fig. 1. It consists of a relatively large reduction δn in the HE photoexcitation density $[\delta n/n(HE) \simeq -3 \times 10^{-3}]$, a smaller increase in the $S^{\pm}$ population at the LE band $[\delta n/n(LE) \simeq 10^{-3}]$, and a EA oscillation that is barely observable in the ADMR spectrum, in agreement with the small value of $\delta n/n(LE)$. Moreover, the δn signals at the LE and HE bands are correlated with each other as verified by studying the dependencies of δn on the pump excitation intensity I_L, sample temperature Θ, and the rf modulation frequency f. In addition to having the same H-ADMR spectrum (Fig. 1, inset), δn for both LE and HE bands increases with I_L as $\delta n \sim I_L^{0.65}$. Also both δn signals decrease with f in the same way, and at $f = 500$ Hz, $\delta n(HE)$ and $\delta n(LE)$ have the same phase lag in the lock-in amplifier. In particular, Fig. 2 shows the PM and ADMR temperature dependencies of the two PA bands. Whereas in the PM spectrum the HE and the LE PA bands do not decrease with Θ in the same way; their δn signals, however, decrease with Θ, together. The experimental correlation between the two δn signals shows, therefore, that a part of the photogenerated $S^{\pm}$ in t-$(CH)_x$ is correlated with the HE species, in spite of their many distinct different properties in the PM spectrum [16].

Recent careful light-induced ESR (LESR) studies [19] of t-$(CH)_x$ showed conclusively the photogeneration of spin-$\frac{1}{2}$ species. It was also speculated [19,20] that these are neutral solitons S^0 associated with the HE band; our ADMR results provide the experimental proof. In fact, we show that the HE band is due to neutral spin-$\frac{1}{2}$ photoexcitations that are correlated with $S^{\pm}$. We conjecture, therefore, that the HE band is due to photogenerated S^0. However, neutral solitons cannot be directly pho-
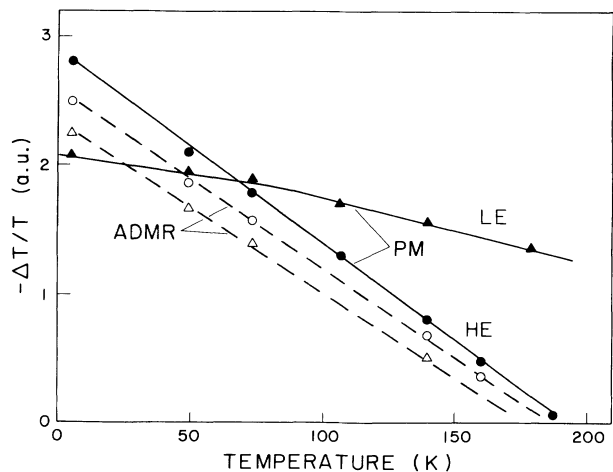

FIG. 1. PM spectrum (solid line) and P-ADMR spectrum (broken line) at 1067 G of t-$(CH)_x$ at 4 K. Inset: The H-ADMR spectrum at 1.35 eV (HE peak). The ADMR resolution is 3×10^{-8} for $\hbar\omega > 1.1$ eV, 6×10^{-8} for $0.8 < \hbar\omega < 1.1$ eV, and 2×10^{-7} for $\hbar\omega < 0.8$ eV.

FIG. 2. The temperature dependencies of the LE and HE PA bands of t-$(CH)_x$ in the PM spectrum (solid lines) and in P-ADMR at 1067 G (broken lines).

togenerated since the photoexcited singlet B_u state cannot decay into a $S^0\bar{S}^0$ pair [10-12]. Either a parity change transition between B_u and $2A_g$ states occurs first [20] and then the $2A_g$ state decays into a $S^0\bar{S}^0$ pair [10-12], or an intersystem crossing from the singlet to the triplet manifold takes place, followed by a triplet exciton fission into a $S^0\bar{S}^0$ pair [21]. In any case the magnitude and sign of δn(HE) indicate that at 4 K the S^0 spins are unthermalized at the rf modulation frequency and that the microwave resonant absorption enhances the recombination kinetics of S^0 by flipping the direction of one S^0 spin $\frac{1}{2}$.

The experimental correlation found between δn(HE) and δn(LE) shows that a conversion process from $S^0\bar{S}^0$ into $S^+\bar{S}^-$ pairs may occur in t-(CH)$_x$, even though $S^0\bar{S}^0$ is the more energetically favorable pair. An important possibility is a fusion process of two $S^0\bar{S}^0$ pairs into an excited $S^+\bar{S}^-$ pair: $2S^0\bar{S}^0 \rightarrow S^+\bar{S}^-$ [22], similar to the fusion process of two triplet excitations into an excited singlet exciton, commonly found in molecular crystals [23]. A different explanation for the positive δn(LE) signal, which does not involve the energetically unfavorable conversion of neutral to charged solitons, is that photogenerated $S^0\bar{S}^0$ pairs act as recombination centers for the long-lived $S^+\bar{S}^-$ pairs, promoting their conversion into $S^0\bar{S}^0$ pairs. Then fewer $S^0\bar{S}^0$ pairs, caused by microwave absorption, may consequently reduce the charged to neutral soliton conversion, resulting in a correlated δn(LE) > 0 signal [22].

The photoexcitation dynamics in polymers with nondegenerate ground state, such as PPV and its alkoxy derivatives, is very different from that of t-(CH)$_x$. Triplet excitons, formed either via the decomposition of the $2A_g$ state [10-12] or through an intersystem crossing from the singlet manifold [21], cannot further produce $S^0\bar{S}^0$ pairs

because of the confinement of the backbone structure [10-12]. We expect therefore that triplet excitons would dominate the PM and ADMR spectra for neutral excitations. This is shown in Fig. 3 for the DOO derivative of PPV at 4 K; we obtained identical results for the DHO derivative. The PM spectrum is composed of two main PA bands: a LE$_1$ band at 0.35 eV and a HE band at 1.36 eV; a shoulder (LE$_2$) is also evident at about 1.3 eV. We have also observed in PPV a strong PL band with 0-0 transition at 2 eV, and this is also shown in Fig. 3. The LE$_1$ and HE PA bands in PPV do not share any common origin as evidenced by their distinct I_L, Θ, and modulation frequency dependencies; the latter is shown as an inset to Fig. 3. In fact the LE$_1$ band is due to charged photoexcitations, whereas the HE band is due to neutral excitations; this was proven by the lack of any ir activity in the phonon spectral range associated with the HE band [24].

The H-ADMR spectrum at 1.36 eV (the HE peak) is shown in Fig. 4 together with the H-PDMR spectrum at 2 eV (the PL peak). We note that the ADMR signal is negative, whereas the PDMR signal is positive [25]. Both spin-dependent spectra, however, show a symmetric band at 1067 G ($g \cong 2.003$) due to spin-$\frac{1}{2}$ excitations and an asymmetric band at 405 G. We identify the later as $\Delta m_s = \pm 2$ transitions associated with triplet excitons having zero field splitting ($D, E \neq 0$) [14,25]. The signal of a triplet "powder pattern" associated with the $\Delta m_s = \pm 1$ transitions, which usually appears together with the $\Delta m_s = \pm 2$ band in the H-ADMR spectrum, was below the noise level for our system equipped with microwaves at 3 GHz. Such a powder pattern signal, however, was recently observed in PDMR measurements of the same PPV derivatives using microwaves at 9 GHz
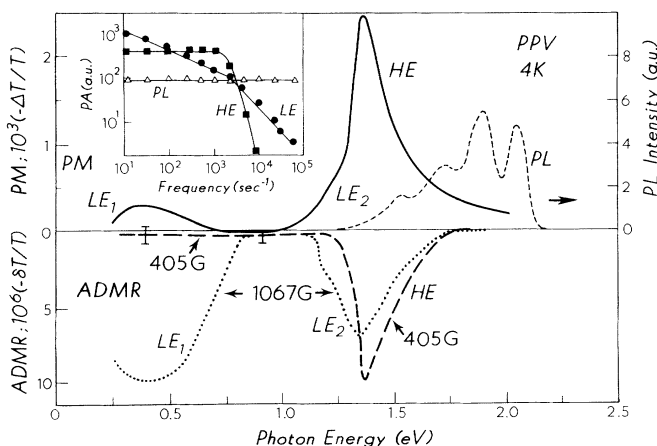

FIG. 3. PM spectrum (solid line) and P-ADMR spectra at 405 G (broken line) and at 1067 G (dotted line), of DOO-PPV at 4 K. The PL band is also shown (right panel) and the different PA bands (LE$_1$, LE$_2$, and HE) are labeled. Inset: The modulation frequency dependencies of the various PA and PL bands up to 10^5 Hz.
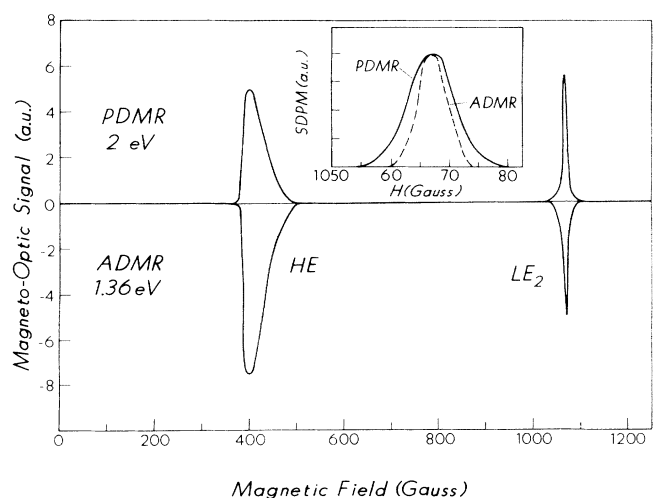

FIG. 4. The H-ADMR and H-PDMR spectra at 1.36 eV (HE band) and 2 eV (PL band), respectively, of DOO-PPV at 4 K. Inset: The two spectra at H around 1067 G are shown in more detail.

[25]; the H-PDMR signal was spread over 1.2 kG and was an order of magnitude smaller than the $g=2$ signal. We have recently succeeded [26] in detecting all three triplet ADMR allowed transitions in *oriented* PPV derivatives at 3 GHz; this was done with H parallel and perpendicular to the chain axis. From our measurements [26], we obtained for the triplet Hamiltonian in PPV, $D=630$ G (0.059 cm^{-1}) and $E=90$ G (0.008 cm^{-1}).

The P-ADMR spectra taken at 1067 G ($S=\frac{1}{2}$) and at 405 G ($S=1$) are shown in Fig. 3. The triplet ADMR spectrum contains a single band peaked at 1.36 eV with the same spectral shape as the HE band in the PM spectrum. The spin-$\frac{1}{2}$ ADMR spectrum, however, contains two bands peaked at 0.3 and 1.3 eV which are equivalent to the LE$_1$ band and LE$_2$ shoulder, respectively, in the PM spectrum. We therefore identify the LE$_1$ and LE$_2$ PA bands as due to optical transitions associated with photogenerated bipolarons (BP$^{2\pm}$), at somewhat lower energies compared to the doping-induced BP [15]. The HE band, on the other hand, is due to optical transitions in the triplet manifold, associated with photogenerated triplet excitons in PPV [24].

The photoexcitation dynamics in PPV, similar to that of t-(CH)$_x$, also shows two competing processes associated with the distinct B_u and $2A_g$ states (or singlet and triplet manifolds). An excited B_u state can decay into spin-$\frac{1}{2}$ polarons ($P^\pm$) [12], which are not topological defects and are therefore relatively mobile in the sample. Although we cannot discern a PA band in the PM spectrum associated with $P^\pm$, their BP$^{2\pm}$ by-products are observable in the PM spectrum. Polaron recombination is a spin-dependent process with faster recombination for polaron pairs with antiparallel spins [14]. This leads to excess $P^\pm$ pair population with parallel spins, which is partially transformed by microwave resonant absorption into $P^\pm$ pairs with antiparallel spins with enhanced recombination. The enhanced $P^\pm$ recombination explains the positive PDMR signal [25] (more PL) and the negative ADMR signal for BP$^{2\pm}$ (LE$_1$ and LE$_2$ in Figs. 3 and 4). This originates from the smaller $P^\pm$ steady-state density under the microwave resonance conditions. On the other hand, if an intersystem crossing from B_u to $2A_g$ (or from the singlet to the triplet manifold) occurs [20], triplet excitons are formed [10-12] with a strong transition at 1.36 eV. These excitons become spin polarized due to different recombination dynamics of each of the triplet sublevels [27]. Under microwave absorption, transitions among the triplet sublevels enhance recombination. This results in a PDMR enhancement and an ADMR reduction due to a decrease in the triplet steady-state population; both changes are in agreement with the measurements presented in Figs. 3 and 4.

(a)Permanent address: Physics Department, California State University, Fresno, CA 93740.

[1] For recent references, see *Proceedings of the International Conference on Science and Technology of Synthetic Metals (ICSM '90)* [Synth. Met. **41-43** (1991)].

[2] A. J. Heeger, S. Kivelson, J. R. Schrieffer, and W. P. Su, Rev. Mod. Phys. **60**, 781 (1988).

[3] K. E. Ziemelis, A. T. Hussain, D. D. C. Bradley, R. H. Friend, J. Ruhe, and G. Wegner, Phys. Rev. Lett. **66**, 2231 (1991).

[4] W. P. Su, J. R. Schrieffer, and A. J. Heeger, Phys. Rev. Lett. **42**, 1698 (1979); Phys. Rev. B **22**, 2099 (1980).

[5] H. Thomann, L. R. Dalton, Y. Tomkiewics, N. S. Shiren, and T. C. Clark, Phys. Rev. Lett. **50**, 553 (1983).

[6] Z. Vardeny and J. Tauc, Phys. Rev. Lett. **54**, 1844 (1985).

[7] D. Baeriswyl and K. Maki, Phys. Rev. B **31**, 6633 (1985).

[8] B. S. Hudson, B. E. Kohler, and K. Schulten, Excited States **6**, 1 (1982).

[9] W.-P. Su, Phys. Rev. B **34**, 2988 (1986); **36**, 6040 (1987).

[10] P. Tavan and K. Schulten, Phys. Rev. B **36**, 4337 (1987).

[11] J. Takimoto and M. Sasai, Phys. Rev. B **39**, 8511 (1989).

[12] G. W. Hayden and E. J. Mele, Phys. Rev. B **34**, 5484 (1986).

[13] J. Orenstein and G. L. Baker, Phys. Rev. Lett. **49**, 1043 (1982).

[14] L. S. Swanson, J. Shinar, and K. Yoshino, Phys. Rev. Lett. **65**, 1140 (1990).

[15] K. F. Voss, C. M. Foster, L. Smilowitz, D. Mihailovic, S. Askari, G. Srdanov, Z. Ni, S. Shi, A. J. Heeger, and F. Wudl, Phys. Rev. B **43**, 5109 (1991).

[16] J. Orenstein, in *Handbook of Conducting Polymers*, edited by T. A. Skotheim (Dekker, New York, 1986).

[17] M. Grabowski, D. Hone, and J. R. Schrieffer, Phys. Rev. B **31**, 7850 (1985).

[18] A. R. Bishop, D. K. Campbell, P. S. Lomdahl, B. Horovitz, and S. R. Philpott, Phys. Rev. Lett. **52**, 671 (1984).

[19] C. G. Levey, D. V. Lang, S. Etemad, G. L. Baker, and J. Orenstein, Synth. Met. **17**, 569 (1987).

[20] S. Kivelson and W.-K. Wu, Phys. Rev. B **34**, 5423 (1986).

[21] W.-P. Su (private communication).

[22] X. Wei and Z. V. Vardeny (to be published).

[23] R. P. Groff, P. Avakian, and R. E. Merrifield, Phys. Rev. B **1**, 815 (1970).

[24] N. F. Colaneri, D. D. C. Bradley, R. H. Friend, P. L. Burn, A. B. Holmes, and C. W. Spangler, Phys. Rev. B **42**, 11670 (1990).

[25] L. S. Swanson, P. Lane, J. Shinar, and F. Wudl, Phys. Rev. B **44**, 10617 (1991).

[26] X. Wei, B. C. Hess, and Z. V. Vardeny, Synth. Met. (to be published).

[27] L. Robins, J. Orenstein, and R. Superfine, Phys. Rev. Lett. **56**, 1850 (1986).